POLITECNICO
MILANO 1863

SCUOLA DI INGEGNERIA INDUSTRIALE
E DELL'INFORMAZIONE

Executive Summary of the Thesis

# Calibration of a cardiac electro-mechanics model in view of Cardiac Resynchronization Therapy

Laurea Magistrale in Mathematical Engineering - Ingegneria Matematica

**Author:** Emilia Capuano

**Advisor:** Prof. Christian Vergara

**Co-advisor:** Simone Stella

**Academic year:** 2021-2022

## 1. Introduction

Cardiac mathematical models describing heart function, either in physiological or pathological conditions, are becoming a potential tool to support therapeutic planning in the clinical context. Given this final goal, it is important to be able to personalize these models [6] exploiting available clinical measurements, in order to study real patient-specific cases.

In this work a patient-specific electromechanical (EM) computational model [4] is employed to virtually reproduce the therapy of cardiac resynchronization (CRT). This clinical treatment aims at restoring a coordinated contraction in dyssynchronous ventricles and improving systolic function in heart failure (HF) patients, by means of a device called *bi-ventricular pacemaker* that sends electrical stimuli to the heart chambers. However, this procedure still needs to be improved, having a 30% of patients that do not respond to the therapy.

The Hospital of S. Maria del Carmine in Rovereto (TN), Italy, provided us with recorded electrical and mechanical data for patients that were implanted with CRT. Our objective is the optimization of the clinical CRT procedure, going on with the work of [3] on three patients, that will be indicated as P2, P5 and P8, all affected by *left bundle branch block* (LBBB), an electrical conduction defect causing a late activation of the left ventricle (LV) and often leading to *ventricular dyssynchrony* (VD). First, the clinical measures are used to reconstruct patients' geometries and to calibrate an EM model able to reproduce the LBBB *pre-operative* behavior of the patients at synus rhythm and subsequently the *clinical* CRT procedure performed by cardiologists. After that, *virtual* CRT scenarios are simulated using the same calibrated model, varying the therapy settings in order to obtain an optimal configuration with respect to the clinical one. The acute beneficial effects of every CRT scenario are evaluated and compared using suitable biomarkers that can be computed from the numerical solution of the EM model.

## 2. Mathematical Model

The electromechanics of the LV is described with the *Eikonal-Reaction-Mechanics* (ERM) model proposed in [4]. The problem is formulated in a LV domain $\Omega \subset \mathbb{R}^3$, with boundary surfaces $\Gamma_{\text{base}}$ for the LV base, $\Gamma_{\text{epi}}$ for the epicardium and $\Gamma_{\text{endo}}$ for the endocardium. The mathematical modelling of each compartment is briefly ad-

dressed below.

**Electrophysiology** (EP) is modelled by a coupled *Reaction-Eikonal* (RE) problem. The *Eikonal-diffusion* equation (1) allows to obtain the activation time $\psi(\boldsymbol{x})$ in every point of the LV myocardium $\Omega$:

$$c_0\sqrt{\nabla\psi\cdot\hat{\mathbf{D}}\nabla\psi}-\varepsilon\nabla\cdot\left(\hat{\mathbf{D}}\nabla\psi\right)=1, \quad (1)$$

where $c_0$ is the velocity of depolarization, $\varepsilon$ is a dimensionless parameter, $\hat{\mathbf{D}}=\frac{\mathbf{D}}{\chi C_m}$ and $\mathbf{D}$ is the conductivity tensor defined as

$$\mathbf{D}=z\sigma_s\mathbf{1}+z(\sigma_f-\sigma_s)\boldsymbol{f}\otimes\boldsymbol{f}+z(\sigma_n-\sigma_s)\boldsymbol{n}\otimes\boldsymbol{n}.$$

Vectors $\boldsymbol{f}$, $\boldsymbol{s}$ and $\boldsymbol{n}$ are the fibers, sheets and normal directions, $\{\sigma_i\}_{i\in\{f,s,n\}}$ are the respective conductivities and $z\in[0,1]$ indicates the degree of fibrosis. The Purkinje network is surrogated by a Dirichlet BC:

$$\psi(\boldsymbol{x})=\psi_a \quad \text{on } S_a\subset\partial\Omega, \quad (2)$$

while on the rest of $\partial\Omega$ homogeneous Neumann BC are imposed.
We will denote this problem with:

$$\psi=\mathcal{E}(\psi_a). \quad (3)$$

The solution $\psi$ is in turn used to solve the *Reaction* equation for the calcium concentration

$$[Ca^{2+}]_i=\mathcal{R}(\psi), \quad (4)$$

which is a simplified version of the monodomain equation (the diffusion term is neglected) coupled to a suitable ionic model.

**Mechanics** is modelled with Finite Elasticity equations that are able to manage the large displacements of the myocardium. The mechanical contraction of the heart muscle is triggered by the electrical propagation through the so called *excitation-contraction* coupling process, leading to the generation of an active force. Such mechanical activation is described by the *RDQ20-MF* model (5) which takes as input the solution of the Reaction problem (4):

$$T_a=\mathcal{F}([Ca^{2+}]_i,\boldsymbol{d}). \quad (5)$$

The active tension $T_a$ depends itself on the displacement $\boldsymbol{d}$, modelled with the following Finite Elasticity equation:

$$\rho\frac{\partial^2\boldsymbol{d}}{\partial t^2}-\nabla\cdot\mathbf{P}(\boldsymbol{d},T_a)=0 \quad \text{in } \Omega\times(0,T), \quad (6)$$

where $\mathbf{P}(\boldsymbol{d},T_a)$ is the Piola-Kirkhhoff stress tensor given by the sum of the passive stress, described with *Guccione constitutive law*, and the active stress given by $T_a$ and assuming that active contraction happens only in the fibers direction $\boldsymbol{f}$.
Concerning boundary conditions, a suitable modelling of the interaction with the external pericardium is used on $\Gamma_{\text{epi}}$. Instead, on $\Gamma_{\text{base}}$ and $\Gamma_{\text{endo}}$ the interaction with blood flow is included by means of the LV pressure. The compact active/passive mechanics problem is

$$\boldsymbol{d}=\mathcal{M}(T_a,p_{LV},\boldsymbol{d}). \quad (7)$$

**Hemodynamics** is described by a reduced-order 0D model for blood circulation, that provides the value of LV pressure $p_{LV}^{0D}$ at each phase of the cardiac cycle:

$$p_{LV}^{0D}=\mathcal{C}(\boldsymbol{d}).$$

In particular, pressure has the role of Lagrange multiplier during the *isovolumetric contraction* and *relaxation* phases in which Eq. (6) is solved under the constant volume constraint. On the other hand, temporal evolution of $p_{LV}^{0D}(t)$ is modelled during the *ejection* phase using a two-element Windkessel model:

$$C\frac{dp_{LV}^{0D}}{dt}+\frac{1}{R}p_{LV}^{0D}=\frac{dV_{LV}^{3D}}{dt}, \quad (8)$$

where $C$ is the arterial compliance and $R$ is the total peripheral resistance. Finally, $p_{LV}^{0D}$ is linearly increased during the *filling* phase.

## 2.1. Numerical Approximation

All computational methods for the numerical approximation of the ERM mathematical model are implemented in the high-performance `C++` library `life`$^{\texttt{x}}$ (`https://lifex.gitlab.io/lifex`). Each subproblem is discretized in space using the Finite Element Method (FEM) of order 1 on hexahedral meshes (Q1). Two different meshes are genereted with `vmtk` software: a finer one for electrophysiology ($h\simeq 1\ mm$) and a coarser one for mechanics ($h\simeq 4\ mm$).

Time discretization is carried out for the mechanics/hemodynamics coupled problem with the Backward Differentiation Formula (BDF) scheme of order 1 using a time-step $\Delta t = 10^{-4}$. The mechanical activation is actually discretized with a forward Euler scheme and requires a smaller $\Delta t = 2.5 \cdot 10^{-5}$ for stability.
In this work we make the simplifying assumption of neglecting the *mechano-electrical feedbacks* avoiding the solution of the electrical problem in a moving domain. This allows to solve once and for all the EP subproblem outside of the temporal loop. Specifically, the personalized Eikonal equation (1) is solved at the beginning of each ERM simulation, while the solution of a generic reduced 0D Reaction problem (4) is obtained off-line for a fixed heartbeat duration of 0.8 $s$ and for every electromechanical simulation it is interpolated in time and evaluated in each mesh point.
We sum up the numerical approximation of ERM model in Algorithm 1, setting $N = \frac{T}{\Delta t}$ to be the number of time-steps, with $T$ final time:

Algorithm 1 ERM numerical approximation

Find $\psi_h$ solving the Eikonal problem (3);
Find $[Ca^{2+}]_{i,h}$ solving the Reaction problem (4);
**for** $0 \leq n \leq N$ **do**
  Interpolate $[Ca^{2+}]_{i,h}$ in time;
  Find $T_{a,h}^{n+1}$ solving the mechanical activation (5) with the finer time-step;
  **if** *isovolumetric contraction* **then**
    Find $(\boldsymbol{d}_h^{n+1}, p_{LV}^{0D,n+1})$ s. t. $V_{LV}^{3D,n+1} = EDV$ and $\boldsymbol{d}_h^{n+1}$ satisfies (7).
    Until $p_{LV}^{0D,n+1} = \bar{p}_{\text{AVO}}^{0D}$;
  **else if** *ejection* **then**
    Solve Windkessel model (8) until $V_{LV}^{3D,n+1} - V_{LV}^{3D,n}$ changes sign;
    Find $\boldsymbol{d}_h^{n+1}$ solution of (7);
  **else if** *isovolumetric relaxation* **then**
    Find $(\boldsymbol{d}_h^{n+1}, p_{LV}^{0D,n+1})$ s. t. $V_{LV}^{3D,n+1} = ESV$ and $\boldsymbol{d}_h^{n+1}$ satisfies (7).
    Until $p_{LV}^{0D,n+1} = \bar{p}_{\text{MVO}}^{0D}$;
  **else if** *filling* **then**
    Linearly increase $p_{LV}^{0D,n+1}$ until $p_{LV}^{0D,n+1} = \bar{p}_{\text{ED}}^{0D}$;
    Find $\boldsymbol{d}_h^{n+1}$ solution of (7).
  **end if**
**end for**

## 3. Patient-specific ERM model

The calibration of the ERM model described in Section 2, exploiting clinical data of patients P2, P5 and P8, is made on three levels: geometric, electrical and mechanical. The geometric and mechanical measurements were obtained with Magnetic Resonance Imaging (MRI) techniques, while recordings of electrical activity come from the *EnSite Precision*$^{TM}$ Electro-Anatomical Mapping System (EAMS).

### 3.1. Geometries

The LV volumes were reconstructed in [3] using a semi-automatic segmentation procedure of MRI images obtained from Hospital of S. Maria del Carmine. Then, using `vmtk` software we obtained the coarse computational mesh for each patient, reported in Figure 1. The same mesh is automatically refined for EP simulations within the ERM code implemented in `life`$^{\text{x}}$.

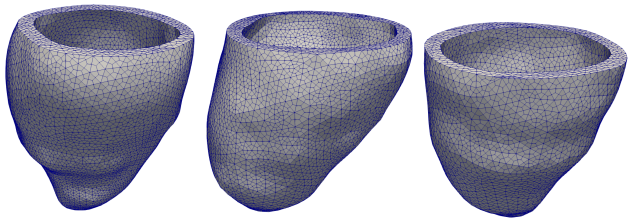

(a) P2 (b) P5 (c) P8

Figure 1: Coarse hexahedral meshes for mechanics generated for patients P2 ($\bar{h} = 3.7\ mm$), P5 ($\bar{h} = 3.6\ mm$) and P8 ($\bar{h} = 3.5\ mm$).

Moreover, patients P5 and P8 were diagnosed with fibrosis and from clinical bullseye plots, the 3D distribution of fibrotic tissue could be reconstructed in [3].
The last important geometric information is the orientation of myocardial fibers, needed to compute the conductivity tensor $\mathbf{D}$ in the Eikonal equation (1). Since fibers geometry can not be detected with MRI, the *Bayer-Blake-Plank-Trayanova* (BT) rule-based algorithm is used, imposing the same boundary values of fibers and sheets orientations on epicardium and endocardium for all the three patients.

### 3.2. Electrical calibration

The personalization of the Eikonal model (1) is carried out starting from measures of activation times (ATs) at the interventricular septum and at the coronary sinus (CS) and its branches [7], acquired at the Hospital of S. Maria del Carmine. The former data, only available for P2 and P5, are used as input $\psi_a$, while the latter serve as target for the estimation of patient-specific $\{\sigma_i\}_{i\in\{f,s,n\}}$, $c_0$ and $\varepsilon$. Concerning P5 and P8, also the degree of fibrosis $z$ is adjusted, indicating the factor by which conduction is reduced in fibrotic regions. The calibrated Eikonal parameters are reported in Table 2, together with mechanical ones. The electrical calibration for each patient consists in performing several Eikonal simulations (taking $\sim$ 5 minutes each) minimizing the relative error between measured and simulated ATs [5]. The final activation maps resulting from the procedure are represented in Figure 2, in which for each patient we report the minimal relative error.

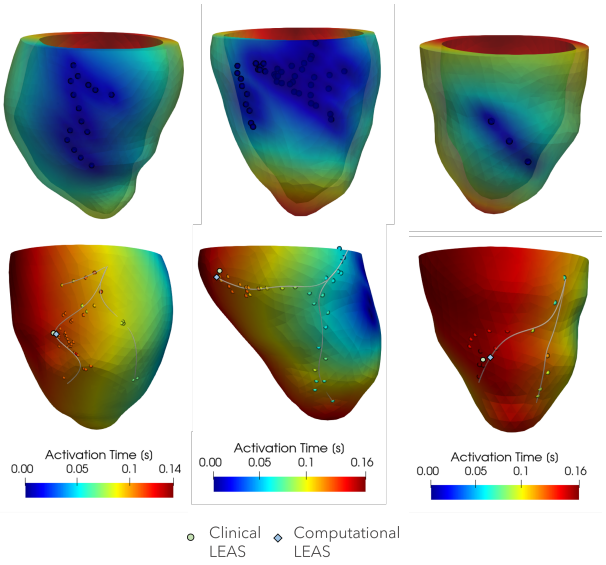


(a) P2: $e = 3.99\%$ (b) P5: $e = 4.51\%$ (c) P8: $e = 9.89\%$

Figure 2: Calibrated activation maps of the *pre-operative* scenario. *Top:* septum stimulation using clinical data only for P2 and P5. *Bottom:* Comparison between simulated and measured ATs at the epicardial veins.

Moreover, we represent the clinical data as bullets and the reconstructed coronary veins along the LV surfaces, obtained interpolating the recorded points at epicardial vessels. The coronary veins geometry is used to identify the latest electrically activated segment (LEAS) as the mesh point with higher AT along the veins. Its location is also reported in Figure 2 where it is compared with the clinical LEAS. We remark that for patient P8 septal recordings were not available, therefore we imposed three stimuli to surrogate the initiation of electrical propagation.

### 3.3. Mechanical calibration

The personalization of the mechanics/0D hemodynamics coupled problem on patients P2, P5 and P8 makes use of MRI measurements of end systolic and end diastolic volumes, $ESV$ and $EDV$, and recordings of systolic and diastolic pressures, being the pressures of aortic valve closing $P_{\text{AVC}}$ and aortic valve opening $P_{\text{AVO}}$, respectively. The clinical measures, all obtained at the Hospital in Rovereto, are reported in Table 1, in which pressure values of patient P5 are not available. The mechanical parameters of *cross-bridge stiffness* $a_{\text{XB}}$ for the mechanical activation (5), of *peripheral resistance* $R$, $\bar{p}^{0D}_{\text{AVO}}$ and $EDV_{init}$ (inital $EDV$) for the 0D Windkessel model (8), are adjusted using the clinical $P_{\text{AVO}}$ as input for $\bar{p}^{0D}_{\text{AVO}}$, and the other three clinical measures as target values to be matched running ERM simulations (taking $\sim 7-8$ hours each), whose final parameters are in Table 2. The resulting patient-specific model is able to perfectly reproduce all mechanical measurements, as it is shown in Table 1. Concerning lacking of P5 pressures, the reference parameter $\bar{p}^{0D}_{\text{AVO}}$ used in [4] is employed and no attention is payed on the value of $P_{\text{AVC}}$, even if this leads to extremely non-physiological values.

| | Data | ESV $[mL]$ | EDV $[mL]$ | $P_{\text{AVO}}$ $[mmHg]$ | $P_{\text{AVC}}$ $[mmHg]$ |
|---|---|---|---|---|---|
| **P2** | *Clinical* | 425 | 501 | 60 | 110 |
| | *Simulated* | 426 | 501 | 60 | 110 |
| **P5** | *Clinical* | 215 | 294 | – | – |
| | *Simulated* | 215 | 294 | 83 | 164 |
| **P8** | *Clinical* | 143 | 214 | 71 | 130 |
| | *Simulated* | 143 | 214 | 70 | 130 |

Table 1: Comparison between clinical and computational mechanical data of volumes and pressures for patients P2, P5 and P8.

We graphically represent the pressure-volume

evolution in the LV during a cardiac cycle, after the ERM model is calibrated, through the so called *PV-loop*. It is reported in Figure 3 for each patient, highlighting the matched mechanical measurements and also the value of maximum rate of pressure change $dP/dt|_{\max}$, that is an important biomarker to assess acute CRT outcomes, being a surrogate for contractility.

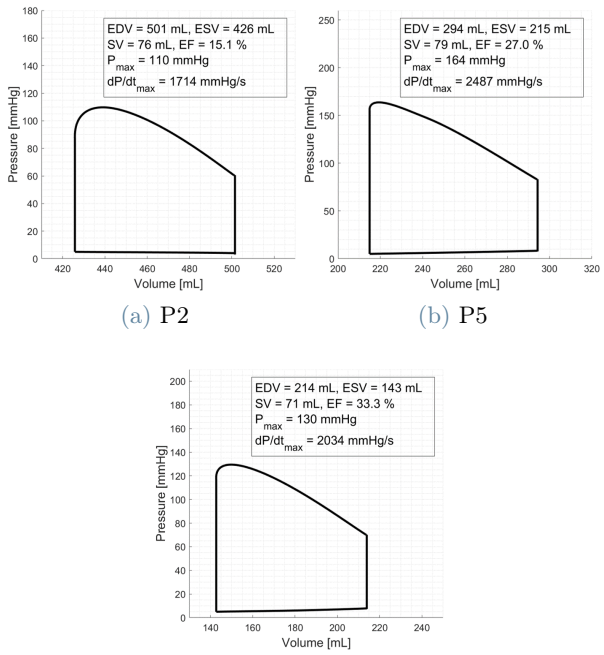


(a) P2 (b) P5

(c) P8

Figure 3: PV-loops obtained after calibration of the ERM model: *pre-operative* scenario.

### 3.4. Final remarks on calibration

We summarize the calibrated electrical and mechanical parameters in Table 2.

| Parameter | P2 | P5 | P8 |
|---|---|---|---|
| $\hat{\sigma}_f$ $[m^2 s^{-1}]$ | $0.23 \cdot 10^{-3}$ | $0.80 \cdot 10^{-4}$ | $0.19 \cdot 10^{-3}$ |
| $\hat{\sigma}_s$ $[m^2 s^{-1}]$ | $0.11 \cdot 10^{-3}$ | $0.37 \cdot 10^{-4}$ | $0.87 \cdot 10^{-4}$ |
| $\hat{\sigma}_n$ $[m^2 s^{-1}]$ | $0.34 \cdot 10^{-4}$ | $0.12 \cdot 10^{-4}$ | $0.28 \cdot 10^{-4}$ |
| $c_0$ $[s^{-\frac{1}{2}}]$ | 84.3672 | 86.5681 | 80.6990 |
| $\varepsilon$ | 11.9602 | 8.9477 | 14.9503 |
| $z$ | 1.0 | 0.6 | 0.7 |
| $a_{\mathrm{XB}}$ $[MPa]$ | $5.2 \cdot 10^2$ | $7.6 \cdot 10^2$ | $3.2 \cdot 10^2$ |
| $\bar{p}^{0D}_{\mathrm{AVO}}$ $[mmHg]$ | 60 | 83 | 70 |
| $EDV_{init}$ $[mL]$ | 464 | 284 | 215 |
| $R$ $[Pa\ s\ m^{-3}]$ | $3.5 \cdot 10^7$ | $8.0 \cdot 10^7$ | $6.3 \cdot 10^7$ |

Table 2: Calibrated ERM parameters. *First group:* electrophysiology. *Second group:* Mechanical activation *RDQ20-MF*. *Third group:* 0D Windkessel model.

The patient-specific ERM models describe the *pre-operative* scenario, because they reproduce the patients' LV function before CRT is implanted, representing the typical electrical propagation of LBBB pathology (Figure 2), the reduced EF (Figure 3) and the mechanical dyssynchrony, that make them candidates for CRT.

## 4. Results of CRT simulations

The CRT implant consists of a device sending electrical signals and three wires, called *leads*, that transmit them to the right atrium (RA), right ventricle (RV) and left ventricle (LV). The *inter-ventricular delay* (VVD) is defined as the time interval between the impulse departure from the right and left leads: VVD $> 0$ indicates RV pre-activation. The EM behavior of a LV undergoing CRT is simulated using the calibrated ERM model (Table 2), modifying the Eikonal BC (2) to impose the RV and LV stimulations. The right stimulus is positioned on the LV epicardial septal region, close to the apex, to surrogate the RV apical electrode, while the left stimulus is located along the reconstructed epicardial veins. Left lead location and VVD settings, key factors for the optimization of the procedure [1], are varied to obtain several CRT *virtual* scenarios, that are compared with each other using as main biomarker the maximum rate of pressure change $dP/dt|_{\max}$ [2] and, eventually, the stroke volume $SV$ and the ejection fraction $EF$.

### 4.1. Simulation of clinical CRT

We first simulate the clinical *LEAS-based* CRT procedure for patients P2, P5 and P8, positioning the left lead at the computational LEAS (see Figure 2). Three different VVDs $= 0, 15, 30$ $ms$ are successively imposed.

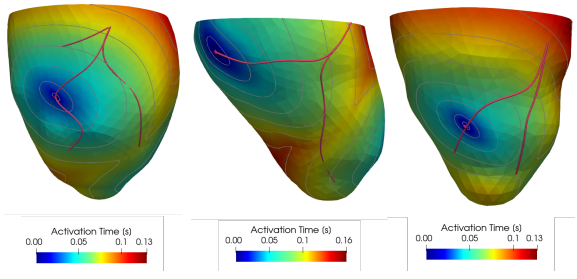


(a) P2 (b) P5 (c) P8

Figure 4: Activation maps of the *LEAS-based* CRT scenario, with VVD $= 0$.

The results of the Eikonal simulations are reported in Figure 4 for the VVD = 0 case. In addition, a comparison of the qualitative mechanical behaviors is presented in Figure 5, highlighting the ability of the simulated clinical CRT to restore a more synchronized ventricular motion.

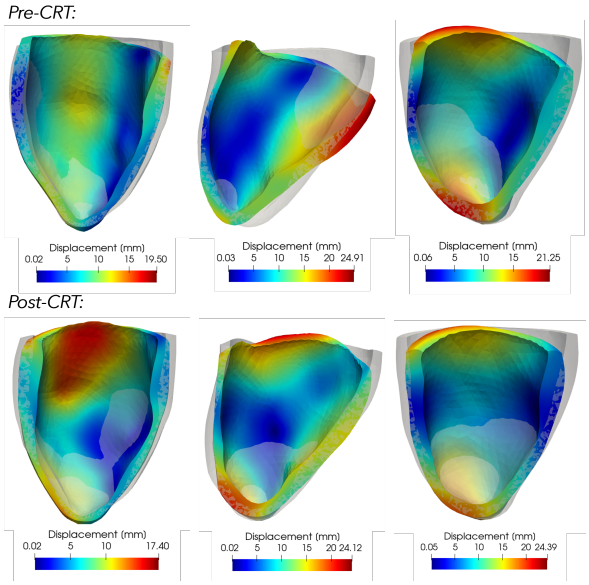


(a) P2 (b) P5 (c) P8

Figure 5: Frame of the myocardial displacement at an intermediate time of the cardiac cycle. *Top: pre-operative* dyssyncrhonous behavior. *Bottom:* Synchronized *LEAS-based* CRT behavior.

## 4.2. Optimization of CRT virtual scenarios

For each patient, potential left lead positions are chosen along the reconstructed veins (Figure 6).

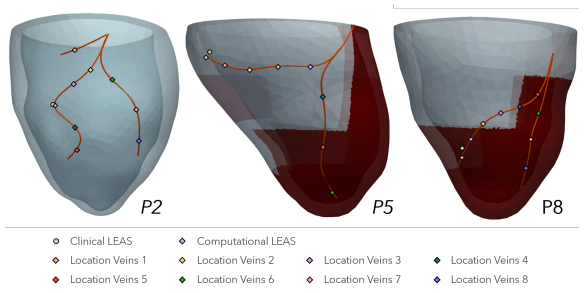


Figure 6: Locations of the LV lead for *virtual* CRT scenarios. Dark regions in P5 and P8 represent the fibrotic tissue.

Every selected point is used as LV pacing site to simulate a CRT *virtual* scenario, setting VVD = 0. Then, based on the best improvements of $dP/dt|_{\max}$ with respect to the *pre-operative* case, 2/3 points per patient are further analyzed imposing a range of VVDs going from $-30$ $ms$ to 60 $ms$, with a step of $10-15$ $ms$. We report in Table 3 the percentage change of biomarkers for the *LEAS-based* and the best CRT *virtual* scenarios.

| | Pacing Site | VVD [$ms$] | $\Delta(dP/dt)$ [%] | $\Delta$(SV) [%] | $\Delta$(EF) [%] |
|---|---|---|---|---|---|
| **P2** | *LEAS* | 0 | +4.6 | +14.5 | +2.1 |
| | *Veins 2* | 20 | +10.6 | +15.8 | +2.3 |
| | *Veins 6* | 20 | +12.9 | +14.5 | +2.2 |
| | *Veins 7* | 10 | +14.7 | +13.2 | +1.9 |
| **P5** | *LEAS* | 0 | +11.7 | +13.9 | +4.0 |
| | *Veins 1* | 60 | +37.7 | +17.7 | +5.2 |
| | *Veins 2* | 40 | +31.4 | +21.5 | +6.0 |
| **P8** | *LEAS* | 0 | −0.9 | +2.8 | +0.8 |
| | *Veins 6* | 20 | +2.8 | +4.2 | +1.2 |
| | *Veins 8* | 10 | +2.9 | −1.4 | −0.4 |

Table 3: Biomarkers corresponding to *LEAS-based* and best CRT *virtual* scenarios.

The *PV-loops*, obtained comparing the different cases of Table 3, are instead in Figure 7.

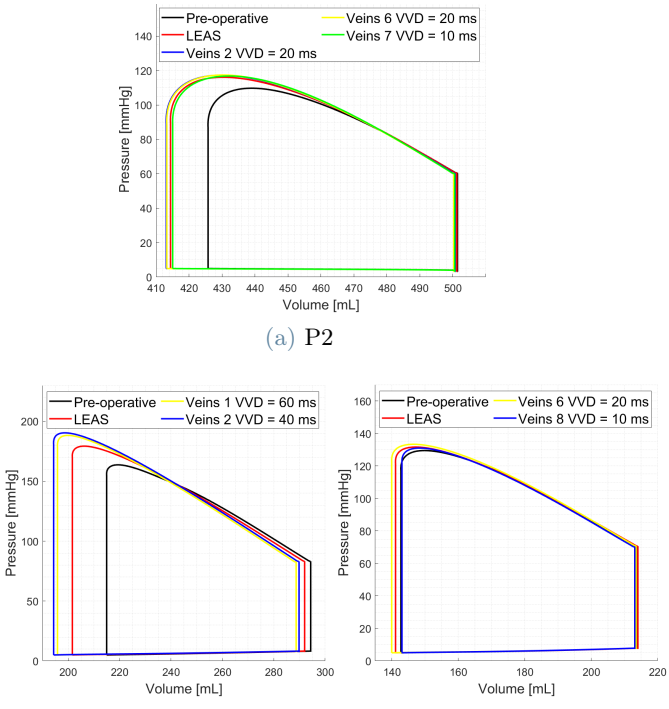


(a) P2

(b) P5 (c) P8

Figure 7: PV-loops comparison among *pre-operative* and *optimal virtual* CRT scenarios.

The combination of left lead position and VVD setting leading to higher $dP/dt|_{\max}$ is identified as the *optimal* CRT scenario for every patient: *Veins 1* for P5 in the basal portion of the lateral surface, *Veins 7* for P2 and *Veins 6* for P8, both in the mid portion of the anterior surface of the ventricle. The corresponding qualitative mechanical behaviors are very similar to those of *LEAS-based* CRT (see Figure 5).

### 4.3. Final remarks

With our CRT simulations we were able to find better locations to be used as pacing sites instead of LEAS, even if the relative increases of the biomarkers were very different between patients. For instance, results for P8 do not reflect a great beneficial effect of the therapy. Moreover, in all cases a higher VVD entailed a greater improvement of $dP/dt|_{\max}$. Finally, based on our results on fibrotic patients P5 and P8, choosing a location for the left lead inside the ischemic region did not affect the acute outcomes of CRT.

## 5. Conclusions

The first objective of the work, regarding the complete patient-specific calibration of the ERM model has been accomplished, employing for the first time all available clinical data in the computational framework.
Secondly, the ability of the model to virtually reproduce and predict the response of each patient to CRT has been established, determining *virtual* scenarios that could be more beneficial than the usual *clinical* procedure. This work represents a first attempt towards the employment of a cardiac computational model in daily clinical practice, aiming at supporting CRT planning for outcomes optimization, thanks to the personalization of therapy settings on the patient, and reducing invasiveness of the procedure.
The methods proposed in this thesis naturally have some limitations that can be overcome with future developments to make them more accurate and reliable.

## References

[1] Angela W. C. Lee, Andrew Crozier, Eoin R. Hyde, Pablo Lamata, et al. Biophysical modeling to determine the optimization of left ventricular pacing site and av/vv delays in the acute and chronic phase of cardiac resynchronization therapy. *Journal of Cardiovascular Electrophysiology*, 28(2):208–215, 2017.

[2] M. Sermesant, R. Chabiniok, P. Chinchapatnam, T. Mansi, et al. Patient-specific electromechanical models of the heart for the prediction of pacing acute effects in crt: A preliminary clinical validation. *Medical Image Analysis*, 16(1):201–215, 2011.

[3] Simone Stella. *Data-driven mathematical and numerical models for the ventricular electromechanics with application to cardiac resynchronization therapy*. PhD thesis, Politecnico di Milano, 2021.

[4] Simone Stella, Francesco Regazzoni, Christian Vergara, Luca Dedè, and Alfio Quarteroni. A fast cardiac electromechanics model coupling the eikonal and the nonlinear mechanics equations. *MOX-Report*, 59:1–24, 2021.

[5] Simone Stella, Christian Vergara, Massimiliano Maines, Domenico Catanzariti, Pasquale Claudio Africa, Cristina Demattè, Maurizio Centonze, Fabio Nobile, Maurizio Del Greco, and Alfio Quarteroni. Integration of activation maps of epicardial veins in computational cardiac electrophysiology. *Computers in Biology and Medicine*, 127:104047, 2020.

[6] Marina Strocchi, Christoph M. Augustin, Matthias A. F. Gsell, Elias Karabelas, et al. A publicly available virtual cohort of four-chamber heart meshes for cardiac electromechanics simulations. *PLOS ONE*, 15(6):1–26, 2020.

[7] C. Vergara, S. Stella, M. Maines, D. Catanzariti, C. Demattè, M. Centonze, F. Nobile, A. Quarteroni, and M. Del Greco. Computational electrophysiology to support the mapping of coronary sinus branches for cardiac resynchronization therapy. *MOX-Report*, 84:1–24, 2020.